Effect of surface roughness on the secondary ion yield in ion sputtering

Maxim A. Makeev and Albert-László Barabási[a)]
Department of Physics, University of Notre Dame, Notre Dame, Indiana 46556

(Received 21 May 1998; accepted for publication 10 July 1998)

There is extensive experimental evidence that, at low temperatures, surface erosion by ion bombardment roughens the sputtered substrate, leading to a self-affine surface. These changes in the surface morphology also modify the secondary ion yield. Here, we calculate analytically the secondary ion yield in terms of parameters characterizing the sputtering process and the interface roughness. © *1998 American Institute of Physics.* [S0003-6951(98)04036-4]

Sputtering is a basic tool in surface analysis and cleaning, depth profiling, and sputter deposition.[1] Due to its widespread use, the effect of the sputtering process on the surface morphology motivated a number of experimental and theoretical investigations. As a result, there is extensive experimental evidence that ion sputtered surfaces either have a self-affine profile[2–6] or, if there is considerable surface diffusion, they may develop a ripple morphology.[7,8] The rough morphology can be described in terms of surface width, $w(\mathbf{r}_\perp,\xi)$, that scales as

$$w^2(\mathbf{r}_\perp,\xi)\equiv\langle[h(\mathbf{r}_\perp)-\overline{h}(0)]^2\rangle=w_{\mathrm{sat}}^2\left(\frac{r_\perp}{\xi}\right)^{2\alpha}f(r_\perp/\xi), \tag{1}$$

where $\mathbf{r}_\perp=(x,y)$, α is the roughness exponent for the interface $h(\mathbf{r}_\perp)$, $h(0)$ is the mean height of the interface, and $\langle\,\rangle$ denotes both ensemble and space average. The scaling function f has the following properties: $f(u\to 0)=1$ and $f(u\to\infty)=u^{-2\alpha}$. The correlation length ξ in Eq. (1) depends on time as $\xi\sim t^{1/z}$, where z is the dynamical exponent.[9]

The experimental relevance of this scaling relation has been verified by experiments involving 5 keV Ar bombarded graphite[2] and iron surfaces,[5] and 0.5 keV Ar ion-bombarded Si surfaces.[6] Motivated by these experimental studies, analytical investigations have addressed the basic mechanisms determining both the rough and the ripple morphologies.[8,10,11]

Uncovering the morphological features of ion-bombarded surfaces leads to the important and still unexplored question: How does roughness affect the sputtering process? The classical theoretical literature focusing on ion sputtering assumes the existence of a *flat surface*, ignoring the surface roughness. Exceptions include the work by Yamamura *et al.*,[12] who studied the sputtering yield for rough surfaces using the Monte Carlo code ACAT. However, their model of a rough surface had a regular comb shape, in contrast with the random self-affine interface morphology uncovered by recent experiments.

In this paper we take a first step toward a systematic understanding of the effect of the surface morphology on the sputtering yield. In agreement with experiments we consider that the bombarded surface is *self-affine*,[9,13] characterized by a well-defined surface width and correlation length, and derive an expression that provides the yield as a function of the experimental parameters characterizing both the ion bombardment and the surface morphology. A combination of numerical and analytical methods is used to investigate the obtained expression and uncover the behavior of the yield. We find that for the experimentally most relevant parameter range the roughness modifies the yield. In particular, we show that the flat-surface approximation (used in all previous analytical studies) is valid only when the penetration depth of the ion is much larger than the surface width.

The physical process taking place during ion bombardment is illustrated in Fig. 1. An ion strikes the surface at point $\mathbf{r}=(x,y,h)$, and stops at a distance a after all its energy is dissipated due to elastic and nonelastic interactions with the atoms of the material. The energy deposited at point $\mathbf{r}_0=(0,0,0)$ by the ion reaching the point $\mathbf{r}=(x,y,z)$ is well described by the Gaussian distribution[14]

$$E(\mathbf{r}_\perp,z)=\frac{\epsilon}{(2\pi)^{3/2}\sigma\mu^2}\exp\left\{-\frac{z^2}{2\sigma^2}-\frac{x^2+y^2}{2\mu^2}\right\}, \tag{2}$$

where ϵ is the kinetic energy of an incident ion and the material-dependent parameters σ and μ characterize the widths of the energy distribution along z and $x(y)$ directions, respectively.

The *erosion rate* at an arbitrary point A on the surface is proportional to the energy deposited by all the bombarding ions. The contributions in the total energy at point A come

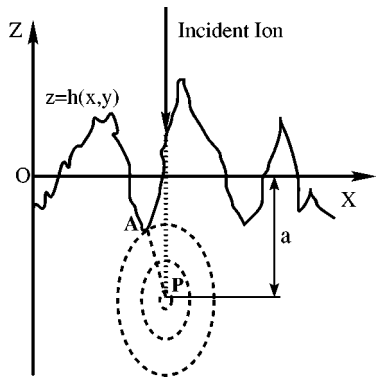

FIG. 1. Following a straight trajectory (the solid line) the ion penetrates an average distance a inside the solid (the dotted line) after which it spreads out its kinetic energy. The energy decreases with the distance from P, the dotted curves indicating schematically the equal energy contours. The energy released at P contributes to erosion at A.

[a)]Electronic mail: alb@nd.edu

from all the points of the substrate R where the ions stop and spread out their kinetic energy, according to Eq. (2). Thus, neglecting the effects of shadowing and redeposition of the eroded material, we obtain the following expression for the normal velocity of erosion at A:

$$v=\lambda \int \int_{\mathscr{R}} d\mathbf{r}_\perp dz E(\mathbf{r}_\perp,z)\Phi(\mathbf{r}_\perp,z). \tag{3}$$

Here the constant λ depends on the properties of the substrate[14–16] and $\Phi(\mathbf{r}_\perp,z)$ is the local correction to the uniform flux J due to local curvature variations.[8]

Following Sigmund[11,14] we assume the following expression for the secondary ion yield:

$$Y=\frac{vn}{\langle \Phi(\mathbf{r}_\perp,z)\rangle}, \tag{4}$$

where n is the density of the target atoms. Limiting the calculations to the case of normal incidence, we obtain the following expression for the local flux variation (due to local curvature):

$$\Phi(\mathbf{r}_\perp,z)=J\cos\{\arctan(\sqrt{[\nabla_x h(x,y)]^2+[\nabla_y h(x,y)]^2})\}. \tag{5}$$

The *exact shape* of the self-affine interface cannot be expressed as a simple analytical function. However, we can use probabilistic concepts and the properties of self-affine interfaces to calculate the average yield.[9] The height–height correlation function of a self-affine interface scales as $\langle[h(\mathbf{r}_\perp)-h(\mathbf{r}_{\perp 0})]^2\rangle\sim(|\mathbf{r}_\perp-\mathbf{r}_{\perp 0}|)^{2\alpha}$. Thus, if we choose $h(0,0)=0$, the probability that the surface height at (x,y) is equal to $h(x,y)$ is given by the Gaussian distribution[9]

$$P(\mathbf{r}_\perp,h)=\frac{1}{\sqrt{2\pi w^2(r_\perp,\xi)}}\exp\left\{-\frac{h^2}{2w^2(r_\perp,\xi)}\right\}, \tag{6}$$

where $w(\mathbf{r}_\perp,\xi)$ is the interface width. Consequently, instead of performing the integral (2) over a well-defined surface topology $h(x,y)$, we take an *average over all possible configurations*, weighting each of them with probability $P(\mathbf{r}_\perp,h)$. Thus we arrive at the following expression for the average yield:[17]

$$Y=\frac{\lambda nJ}{\langle \Phi(\mathbf{r}_\perp,z)\rangle}\int_{\mathscr{R}}\int_{-\infty}^{\infty} d\mathbf{r}_\perp dh E(\mathbf{r}_\perp,h)P(\mathbf{r}_\perp,h)\langle\Phi(\mathbf{r}_\perp,h)\rangle. \tag{7}$$

Next we assume that the probability distribution of the height $P(\mathbf{r}_\perp,h)$ and the probability distribution of the height gradient $P[\mathbf{r}_\perp|\nabla_x z(x,y),\ \nabla_y z(x,y)]$ are decoupled, which is consistent with the random, i.e., self-affine nature of rough interfaces. Using Eqs. (2)–(7) and performing the integral over h we obtain the yield as

$$Y=\frac{\lambda n\epsilon}{(2\pi)^{1/2}\mu^2}\int_0^\infty r dr\ \frac{1}{\sqrt{(w^2(r,\xi)+\sigma^2)}} \times\exp\left\{-\frac{r^2}{2\mu^2}\right\}\exp\left\{-\frac{a^2}{2(w^2(r,\xi)+\sigma^2)}\right\}. \tag{8}$$

To proceed further, we need to include the functional form of the interface width (1) in Eq. (8). Using Eqs. (1) and (8), we finally obtain the yield as a sum of two integrals

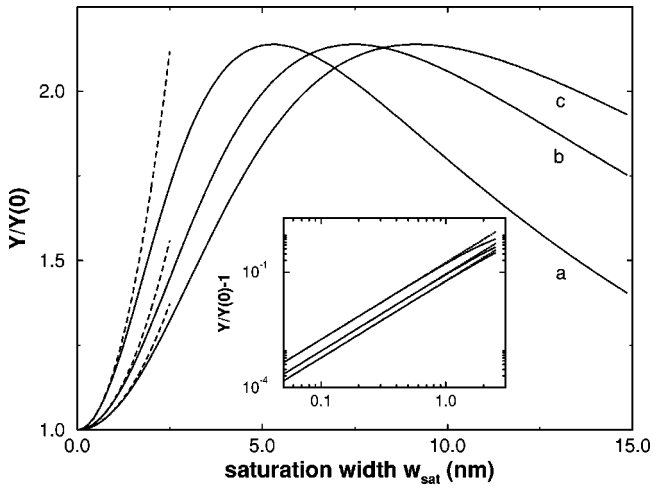

FIG. 2. Normalized yield as a function of the saturation width, w_{sat}. We used $\xi=21$ nm, and the different curves correspond to penetration depths a equal to (a) 0.5 nm, (b) 1 nm, and (c) 1.5 nm. Dashed curves correspond to the parameter free small w_{sat}/a expansion of Eq. (9), given by Eq. (12). The inset shows the normalized yield $(Y/Y(0)-1)$ on a log–log scale for small values of w_{sat}/a, emphasizing the good agreement between the expansion and Eq. (12).

$$Y=\left(\frac{\lambda n\epsilon}{(2\pi)^{1/2}\mu^2}\right)(I_1+I_2), \tag{9}$$

$$I_1=\int_0^\xi r dr\ \frac{1}{\sqrt{(w_{sat}^2(r/\xi)^{2\alpha}+\sigma^2)}}\exp\left\{-\frac{r^2}{2\mu^2}\right\} \times\exp\left\{-\frac{a^2}{2(w_{sat}^2(r/\xi)^{2\alpha}+\sigma^2)}\right\}, \tag{10}$$

$$I_2=\frac{1}{\sqrt{(w_{sat}^2+\sigma^2)}}\exp\left\{-\frac{a^2}{2(w_{sat}^2+\sigma^2)}\right\}\exp\left\{-\frac{\xi^2}{2\mu^2}\right\}. \tag{11}$$

Equations (9)–(11) completely describe the yield as a function of the parameters characterizing the ion-bombardment process, such as ion penetration depth a, the widths of the deposited energy distributions, μ and σ, and the parameters characterizing the surface morphology, such as the saturation width, w_{sat}, and correlation length ξ. Next we proceed by integrating Eq. (4) numerically for different values of ξ and a.[18]

Figure 2 shows the variation of the total yield with the saturation width w_{sat} for different values of a. This plot allows for direct comparison with experiments since roughness grows with irradiation time as $w_{sat}\sim t^\beta$, providing a direct relation between w_{sat} and the experimentally available irradiation time.

As Fig. 2 illustrates, two leading behaviors can be distinguished.

(a) $w_{sat}\ll a$: In this regime the yield increases with w_{sat}. The origin of this behavior is the following: With an increasing w_{sat} the total area of the surface also increases. If all the sputtering conditions are the same, a larger surface area is known to lead to an increased yield.[19,20] In the limit $\xi\gg w_{sat}$ we can expand Eq. (9) for small w_{sat}/a, keeping terms up to the second order. We find that in the initial stages of the roughening process the yield depends on the saturation width as $Y=Y(0)+Cw_{sat}^2$, the exact expression[21] being

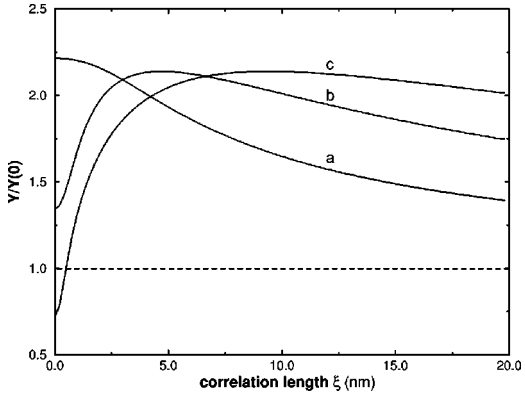

FIG. 3. Normalized yield as a function of the correlation length ξ, plotted for $w_{\mathrm{sat}}=5$ nm. Different curves correspond to different values of the penetration depth, such as (a) $a=5$ nm, (b) $a=2$ nm, and (c) $a=1$ nm. The dashed line corresponds to the flat surface limit.

$$Y=\frac{\lambda n\epsilon}{(2\pi)\sigma}\exp\left\{-\frac{1}{2\epsilon_1^2}\right\}\left[1+\frac{w_{\mathrm{sat}}^2}{a^2}\left(\frac{1}{2\epsilon_1^4}-\frac{1}{2\epsilon_1^2}\right)\times\frac{\sqrt{(2\pi\mu^2)}}{2\xi}\left\{1-\sqrt{\frac{2\mu^2}{\pi\xi^2}}\exp\left\{-\frac{\xi^2}{2\mu^2}\right\}\right\}\right]. \quad (12)$$

As Fig. 2 illustrates, Eq. (12) provides an excellent approximation for small w_{sat}. The experimentally relevant parameter ranges for w_{sat} and ξ span a wide region, depending on the particular realization of sputtering conditions (such as the incident ion energy, ion flux, interface temperature).[2] However, for many systems this quadratic regime in w_{sat} is the most important experimentally. For example in Ref. 2 w_{sat} varies from 0 to 10 nm, and $\xi\sim 0-25$ nm, thus the first 25%–50% of the experimentally available sputtering range is well described by the quadratic law. Furthermore, most technologically relevant sputtering methods require much less erosion, thus these experiments and the entire process will be described by the quadratic law (12).

(b) $w_{\mathrm{sat}}\gg a$: In this regime the yield decreases with w_{sat} following $Y\sim 1/w_{\mathrm{sat}}^2$. As the gradients of height variations grow (corresponding to wider probability distributions of the height) the region R within which the ions contribute to erosion [which is defined by the effective cutoff in the energy distribution function (2)] at O decreases, thus decreasing the average erosion rate.

A second important quantity characterizing the surface roughness (9) is the correlation length. Figure 3 shows the secondary ion yield variations with ξ. As one can see, for $w_{\mathrm{sat}}\leqslant\xi$, the yield decreases with ξ. As Eq. (9) indicates, as ξ grows for fixed w_{sat} and r, the width $w(r,\xi)$ decreases, the scaling function approaching the flat surface limit. Indeed, the yield converges to the flat surface limit for large ξ.[17] Since for rough surfaces[3,9] typically $\xi\geqslant w_{\mathrm{sat}}$, we expect that for the experimentally available sputtering conditions the yield will decrease with ξ. An important consequence of Fig. 3 is that the flat surface approximation, used in all previous analytical and numerical analysis, can be applied only when $\xi\gg w_{\mathrm{sat}}$. However, we find that in the experimentally relevant region $\xi\geqslant w_{\mathrm{sat}}$ there are considerable deviations (up to more than 100%) from the flat surface limit.

In a typical experiment sputtering starts from a relatively smooth surface, which then roughens by ion bombardment. The interface width is expected to increase as $w_{\mathrm{sat}}\sim t^{\beta}$ and $\xi\sim t^{1/z}$. According to our previous discussion, such an increase in the w_{sat} and ξ will result in a modified yield as well. The magnitude of the yield change depends on the interplay between the parameters w_{sat}, ξ, and a, and for a given experiment can be explicitly obtained by integrating Eqs. (9)–(11). Eventually, w_{sat} and ξ reach a saturation value, which is expected to lead to the saturation of the yield as well. The accumulated information on surface roughening,[9,13] combined with Eqs. (9)–(11), allows us to make rather specific predictions on the interplay between the yield and the surface morphology. Since many experimental techniques (e.g., secondary ion mass spectrometry) probing the material structure rely on the precise determination of the secondary ion yield, the understanding of the morphology-induced yield modifications goes beyond mere scientific interest, having a direct technological impact.

This research was partially supported by the Faculty Research Program of the University of Notre Dame.

[1] P. D. Townsend, J. C. Kelly, and N. E. W. Hartley, *Ion Implantation, Sputtering and their Applications* (Academic, London, 1976).
[2] E. A. Eklund, R. Bruinsma, J. Rudnick, and R. S. Williams, Phys. Rev. Lett. **67**, 1759 (1991).
[3] E. A. Eklund, E. J. Snyder, and R. S. Williams, Surf. Sci. **285**, 157 (1993).
[4] H. You, R. P. Chiarello, H. K. Kim, and K. G. Vandervoort, Phys. Rev. Lett. **70**, 2900 (1993).
[5] J. Krim, I. Heyvaert, C. Van Haesendonck, and Y. Bruynseraede, Phys. Rev. Lett. **70**, 57 (1993).
[6] H.-N. Yang, G.-C. Wang, and T.-M. Lu, Phys. Rev. B **50**, 7635 (1994).
[7] E. Chason, T. M. Mayer, B. K. Kellerman, D. N. McIlroy, and A. J. Howard, Phys. Rev. Lett. **72**, 3040 (1994); T. M. Mayer, E. Chason, and A. J. Howard, J. Appl. Phys. **76**, 1633 (1994).
[8] R. Cuerno and A.-L. Barabási, Phys. Rev. Lett. **74**, 4746 (1995); R. Cuerno, H. A. Makse, S. Tomassone, S. T. Harrington, and H. E. Stanley, *ibid.* **75**, 4464 (1995).
[9] A.-L. Barabási and H. E. Stanley, *Fractal Concepts in Surface Growth* (Cambridge University Press, Cambridge, 1995).
[10] M. A. Makeev and A.-L. Barabási, Appl. Phys. Lett. **71**, 2800 (1997).
[11] R. M. Bradley and J. M. E. Harper, J. Vac. Sci. Technol. A **6**, 2390 (1988).
[12] Y. Yamamura, C. Mossner, and H. Oechsner, Radiat. Eff. **103**, 25 (1987).
[13] *Dynamics of Fractal Surfaces*, edited by F. Family and T. Vicsek (World Scientific, Singapore, 1991); P. Meakin, Phys. Rep. **235**, 189 (1993); T. Halpin-Healey and Y.-C. Zhang, *ibid.* **254**, 215 (1995).
[14] P. Sigmund, Phys. Rev. **184**, 383 (1969); J. Mater. Sci. **8**, 1545 (1973).
[15] M. A. Makeev and A.-L. Barabási (unpublished).
[16] M. A. Makeev and A.-L. Barabási, Appl. Phys. Lett. **72**, 906 (1998).
[17] Note that the yield for a flat surface can be obtained from Eq. (7) using $P(x,y)=\delta(h(x,y)-h_0)$.
[18] We used a linear relation between energy distribution widths σ and μ and penetration depth a, i.e., $\sigma=\epsilon_1 a$ and $\mu=\epsilon_2 a$. The coefficients $\epsilon_1=1/2$ and $\epsilon_2=1/4$ are chosen in such a way as to obtain an anisotropic energy distribution (Ref. 1).
[19] The same mechanism for yield modifications has been discussed by Sigmund (Ref. 14) and was used to describe the secondary ion yield changes on rippled interfaces (Refs. 16 and 21).
[20] K. Wittmaak, J. Vac. Sci. Technol. A **8**, 2246 (1990).
[21] Note that a similar quadratic dependence on the width appears for yield changes on rippled interfaces (Ref. 16).